A Water-Soluble Cycloparaphenylene: Synthesis and Application as a Supramolecular Receptor with Visible Fluorescence

Ryo Morito,[a] Takayuki Kataoka,[a] Kunio Saito,[a] Kohtaro Osakada,[b] Tomohito Ide,[c] Yoshitaka Tsuchido,*[a] and Hidetoshi Kawai*[a]

[a] Department of Chemistry, Faculty of Science, Tokyo University of Science, 1–3 Kagurazaka, Shinjuku-ku, Tokyo 162-8601, Japan

E-mail: tsuchido@rs.tus.ac.jp, kawaih@rs.tus.ac.jp

[b] Laboratory for Chemistry and Life Science, Institute of Innovative Research, Tokyo Institute of Technology, 4259, Nagatsuta, Midori-ku, Yokohama 226-8503, Japan

[c] Department of Chemical Science and Engineering, National Institute of Technology, Tokyo College, 1220-2 Kunugida-machi, Hachioji-shi, Tokyo, 193-0997, Japan

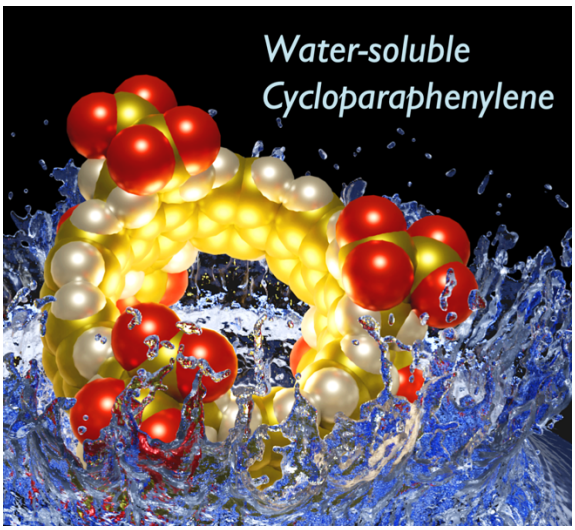

Abstract

We report the first synthesis of water-soluble [9]cycloparaphenylene derivative containing three hydrindacene (1,2,3,5,6,7-hexahydro-*s*-indacene) units with four carboxylates at the 2,6-positions via a macrocyclic gold complex. This crown-shaped macrocyclic compound exhibits remarkable water solubility, with a maximum solubility of 16 mmol L^{-1} (2.6 g/100 mL), as well as strong visible fluorescence in water (λ_{em} = 447 nm, φ_F = 0.64, brightness ($\varepsilon \times \varphi_F$) = 5.1×10^4). This molecule effectively encapsulates cationic guest compounds, such as methyl viologen dichloride, as indicated by a change in visible fluorescence.

Introduction

A water-soluble macrocyclic supramolecular hosts that exhibit fluorescence are of significant interest for their potential applications such as biosensing[1] and drug delivery systems[2] (DDS). Ogoshi et al.[3] and Huang et al.[4] reported the successful water solubilization of pillar[*n*]arenes (*n* = 5, 6) by converting the methoxy groups to carboxylates (-OCH_2COO^-) (Figure 1a, left), and exhibited guest recognition as indicated by a change in an ultraviolet fluorescence. On the other hand, the supramolecular hosts exhibiting visible fluorescence in water typically involve either the immobilization of a fluorophore or inclusion of a fluorescent guest into the macrocyclic structures.[5] A limited number of water-soluble macrocyclic hosts exhibit visible fluorescence directly from their cyclic skeleton, with examples including macrocyclic hosts containing anthracene and pyrene.[6][7] Very recently, Guo and Cai et al. reported that water solubilization of a macrocyclic π-conjugated compound consisting of five diphenylacetylene units linked at the 2,2'-position (corral[5]arene) by introducing sulfate groups at the 4,4'-positions of each units, which selectively forms 1:1 inclusion complexes with various cationic guest molecules in water with extremely high association constants ($K_a \sim 10^{11}$ M^{-1}) (Figure 1a, right).[8]

However, water-soluble supramolecular hosts composed of aromatic rings connected though the methylene or ethynylene units would suffer from reduced fluorescence properties, especially brightness ($\varepsilon \times \Phi_F$) based on fluorescence quantum yield (Φ_F), due to the thermal vibration arising from the molecular flexibility and aggregation[4] induced by the intermolecular dispersion interactions in the aqueous environment.

In this regard, [*n*]cycloparaphenylenes ([*n*]CPPs, where *n* is the number of phenylene groups), which are the macrocyclic organic compounds consisting of 1,4-linked phenylene unit, have attracted significant interest owing to their unique π-conjugated structures and physical properties.[9][10][11] In particular, [7] to [10]CPPs exhibit strong blue to green fluorescence (λ_{em} = 450 – 587 nm, Φ_F = 0.38 – 0.81) and high molar absorption coefficients ($\varepsilon \sim 10^5$ M^{-1} cm^{-1}), as well as having a molecular diameter of 0.95 – 1.6 nm.[10] Unlike polyparaphenylenes (PPPs), [*n*]CPPs dissolve readily in common organic solvents due to the curved benzene rings, which can avoid intermolecular aggregation. Thus, these molecules may serve as promising novel supramolecular hosts with visible fluorescence in aqueous environments, if they can be rendered solubility in water. However, the synthesis of [*n*]CPPs with polar substituents is difficult - the only example of a water-soluble CPP is a [8]CPP derivative with two units of alkoxysulphonate that can dissolve in phosphate-buffered saline (PBS) solution contains 0.1% of the detergent sodium dodecylsulfate (SDS) (Figure 1b), synthesized by Jasti et al. in 2018 as a biosensing material.[12] Thus, there remains no example of a CPP derivative that dissolves in pure water.

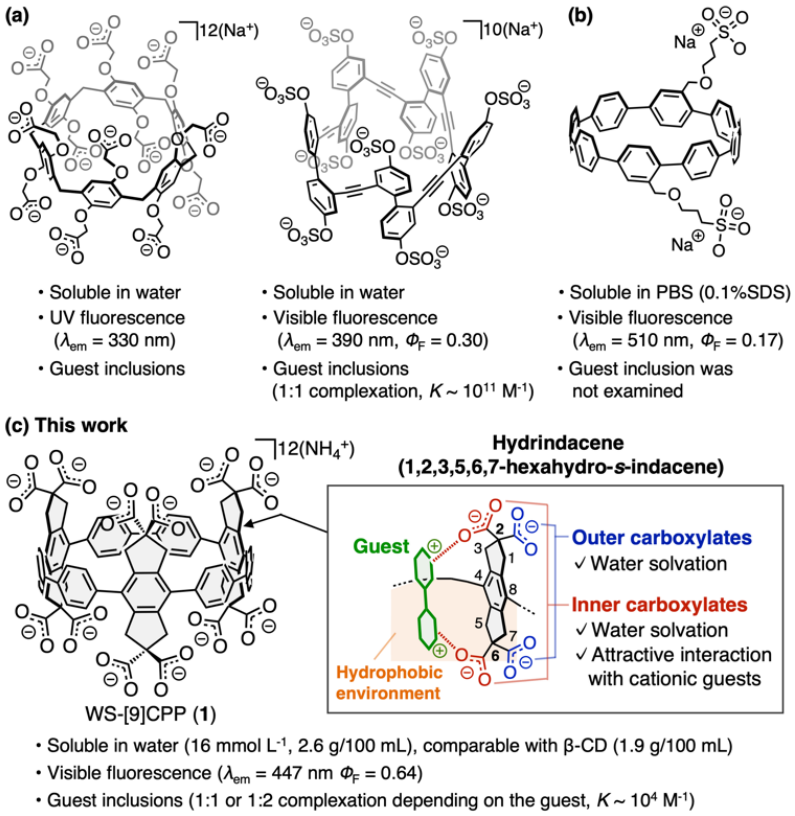

Figure 1. Structures of artificial water-soluble macrocycles. (a) water-soluble pillar[6]arene (left)[4] and water-soluble corral[5]arene (right),[8] (b) [8] cycloparaphenylene derivative with two alkoxysulphonate units.[12] (c) Water-soluble [9]cycloparaphenylene derivative containing three hydrindacene units with four carboxylates at the 2,6-positions (This work).

In this study, we report the first synthesis of water-soluble CPP derivative that exhibit strong visible fluorescence in water and its application as a supramolecular host. To enhance the water solubility of [*n*]CPPs, we utilized a hydrindacene (1,2,3,5,6,7-hexahydro-*s*-indacene) skeleton as a scaffold for the introduction of multiple polar substituents. This hydrocarbone features a molecular structure and high functionality that facilitate the ordered placement of multiple substituents, and we have applied it in the synthesis of hydrindacene-based macrocycles,[13] allosteric receptors,[14-16] and rotaxane molecular shuttles.[17-21]

With the above background, we designed [9]cycloparaphenylene ([9]CPP) derivative (**1**) containing three hydrindacene units with four carboxylates at the tip of the five-membered rings (2,6-positions) (Figure 1c). [9]CPP has a diameter suitable for encapsulating one or two benzene rings and exhibits visible fluorescence. Moreover, the precise positioning of carboxyl groups in close proximity to the CPP framework *via* the hydrindacene unit, oriented both toward the inside and outside of the macroring, not only improves water solubility, but also allows inclusion of guest molecules through attractive interactions with polar groups immobilized in the ring (Figure 1c, inset).

Results and discussion

The synthesis of WS-[9]CPP (**1**) is accomplished through the utilization of our developed CPP synthesis method,[22-24] which employs macrocyclic gold complex (Figure 2a). The initial step involves the preparation of hydrindacene with four ethyl ester groups at the 2,6-positions (**8**)[25] through a double-ring condensation reaction between 1,2,4,5-tetrakis(bromomethyl)benzene (**9**) and diethyl malonate under basic conditions in 63% yield. Despite the 4,8-positions of hydrindacene being less reactive towards halogenation due to the steric hindrance from the methylene protons, successful iodation was achieved through treatment with 1,3-diiodo-5,5-dimethylhydantoin (DIH)[26] under acidic conditions (H_2SO_4/AcOH) resulting in the formation of diiodide (**7**) in 66% yield (see supporting Table S2). The synthesis of a *p*-terphenylene derivative (**6**) was achieved through a Pd-catalyzed Suzuki-Miyaura coupling reaction between **7** and 4-chlorophenylboronic acid in 66% yield. Subsequently, the terminal chloro groups of **6** were converted to boronic esters through a Miyaura borylation reaction with B_2pin_2, thereby yielding the diboronate ester (**5**) in 79% yield. The reaction of **5** with [Au_2Cl_2(dcpm)] (dcpm = bis(dicyclohexylphosphino)methane) in the presence of Cs_2CO_3, yielded the macrocyclic Au complex (**4**) in 81% yield. Then, the oxidative chlorination[27] of **4** was carried out by treatment with $PhICl_2$ to give [9]CPP derivative with twelve ethyl ester groups (**3**) in 60% yield. The molecular structure of compound **3** was confirmed by single crystal X-ray crystallography (Figure 2b and Supporting Figure S50). The final step involved the hydrolysis of the ester groups of **3** followed by treatment with aqueous ammonia resulting in the formation of ammonium carboxylates, yielding WS-[9]CPP (**1**) in 86% yield over 2 steps.

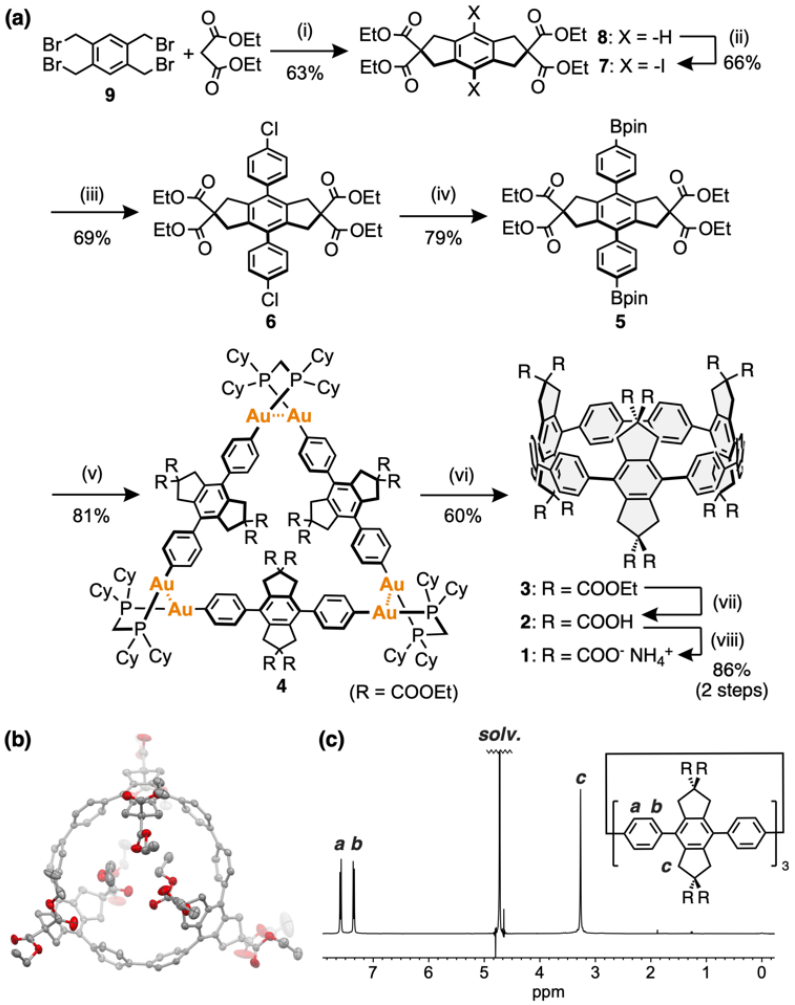

Figure 2. Synthesis and characterization of WS-[9]CPP (**1**): (a) synthetic route for **1**. Reagents and conditions; (i) NaH (5.0 equiv.), THF, 70 ºC, 3 h, (ii) 1,3-diiodo-5,5-dimethylhydantoin (DIH) (1.5 equiv.), H_2SO_4/AcOH, r.t., 15 h, (iii) 4-chlorophenylboronic acid (3.0 equiv.), $Pd(PPh_3)_4$ (6.5 mol%), Na_2CO_3 (6.0 equiv.), toluene/H_2O, 85 ºC, 24 h, (iv) B_2pin_2 (4.0 equiv.), $Pd_2(dba)_3$ $CHCl_3$ (6.3 mol%), XPhos (20 mol%), KOAc (6.0 eq.), 1,4-dioxane, 100 ºC, 15 h, (v) $[Au_2Cl_2(dcpm)]$ (1.0 equiv.), Cs_2CO_3 (6.0 equiv.), toluene/EtOH/H_2O, 50 ºC, 16 h, (vi) $PhICl_2$ (3.0 equiv.), CH_2Cl_2, -60 ºC to r.t., 18 h. (vii) NaOH, THF/H_2O/EtOH, 70 ºC, 21 h, (viii) NH_3 solution (28-30%), H_2O, 5 min. (b) ORTEP drawing of compound **3** (50% level of probability for thermal ellipsoids; gray, carbon; red, oxygen). Hydrogen atoms and solvent molecule are omitted for clarity. (c) ^{1}H NMR spectrum of **1** (400 MHz, D_2O, 298 K).

Surprisingly, despite WS-[9]CPP (**1**) being a rigid π-conjugated organic compound, it shows remarkable solubility in pure water owing to the twelve ammonium carboxylates incorporated into the molecule, with a maximum solubility of 16 mmol L^{-1} (2.6 g/100 mL) at ambient temperature. In comparison to typical water-soluble hosts, the solubility of **1** is 1000-fold greater than that of cucurbit[6]uril (13 μmol L^{-1}, 1.3 mg/100 mL),[28] and comparable to that of cyclodextrins (1.9-23 g/100 mL).[29]

Variable-concentration ^{1}H NMR measurements revealed that **1** did not undergo aggregation within the concentration range from 0.5 mM to 0.05 mM (see Supporting Figure S15). The ^{1}H NMR spectrum of **1** in D_2O shows two aromatic peaks at 7.65 ppm (H_a) and 7.43 ppm (H_b), and one methylene peak at 3.33 ppm (H_c) (Figure 2c). The methylene protons (H_c) were observed as a single peak, although the chemical environment should be different in the inside and the outside of the CPP macroring. This result suggests that the hydrindacene units flip faster than the ^{1}H NMR timescale, around the carbon atoms at the 4,8-positions as a rotational axis (Figure 1c). The variable-temperature ^{1}H NMR measurements of **3** in CD_2Cl_2 observed a splitting of the H_c signals below -65 °C, and the energy barrier of ring flip movement of hydrindacene units was estimated to be $\Delta G^{\ddagger}$ (298) = 9.7 kcal mol^{-1} using the Eyring equation based on the dynamic ^{1}H NMR line-shape simulations (see Supporting Figure S18).

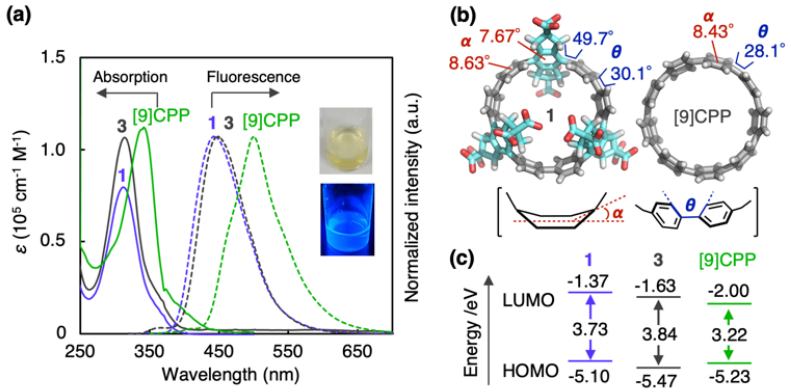

Figure 3. (a) UV/Vis absorption (solid lines) and fluorescence (dotted lines) spectra of WS-[9]CPP (**1**) (blue lines), **3** (black lines), and [9]CPP (green lines) (H_2O for **1**, CH_2Cl_2 for **3** and [9]CPP, [M] = 1.0 x 10^{-6} M, r.t.) (inset: photos of aqueous solution of **1** (top) and of that under UV irradiation (bottom)). (b) Optimized structures of WS-[9]CPP (**1**) (left) and [9]CPP (right) by DFT calculations (SMD-r^{2}SCAN-3c(+ma) level of theory). The values of ring strain (α) and dihedral angle (θ) were determined by averaging over all benzene rings in the molecule. (c) Energy levels of HOMO and LUMO for WS-[9]CPP (**1**) (left), **3** (middle), and [9]CPP (right) (SMD-B3LYP/(ma-)def2-TZVP//SMD-r^{2}SCAN-3c(+ma) level of theory).

WS-[9]CPP (**1**) exhibits an absorption maxima at λ_{max} = 308 nm and an absorption edge at 380 nm in H_2O (Figure 3a, solid lines). This is approximately 30 nm hypsochromic shift relative to [9]CPP in CH_2Cl_2 (λ_{max} = 338 nm). The similar absorption as that of **1** in H_2O was observed in the measurement of **3** in CH_2Cl_2 (λ_{max} = 311 nm), suggesting that the hypsochromic shift in **1** should not be caused by the polarity of the solvent or the electronic effect of the substituents, but to a change in the curved π-conjugated system due to the introduction of the bulky hydrindacene units. The DFT optimized molecular structures using ORCA[30] showed that the averaged Ar-Ar dihedral angle (θ) between the hydrindacene unit and the phenylene ring in **1** (49.7°) became significantly larger than

the angles between the two phenylene rings in both of **1** (30.1°) and [9]CPP (28.1°) due to the steric hindrance of methylene groups in hydrindacene units (Figure 3b). On the other hand, the averaged ring strain (α) of the aryl rings was estimated to be similar for **1** (7.67°, 8.63°) and [9]CPP (8.43 °). In the circularly π-conjugated system of CPPs, increasing the Ar-Ar dihedral angle causes a destabilization of the LUMO levels,[31] which leads to the hypsochromic shift in **1** relative to [9]CPP (Figure 3c). A similar trend was observed in the fluorescence spectra (Figure 3a, dotted lines) of **1** (λ_{em} = 447 nm, φ_F = 0.64, in H_2O) and **3** (λ_{em} = 453 nm, φ_F = 0.77, in CH_2Cl_2) being about 50 nm hypsochromic shift relative to [9]CPP (λ_{em} = 504 nm, φ_F = 0.68, in CH_2Cl_2) due to the large Ar-Ar dihedral angles.[32][33] These results demonstrate that **1** exhibited strong visible fluorescence in water (brightness ($\varepsilon\times\varphi_F$) = 5.1×10^4) even when the multiple substituents are introduced to ensure the water solubility.

To evaluate the guest inclusion ability of WS-[9]CPP(**1**) in aqueous environment, the association with various water-soluble guest molecules was examined (see Supporting Figure S25). It was found that **1** exhibited remarkable inclusion ability towards various bipyridinium salts, such as methyl viologen dichloride (**G1**) (Figure 4a), 4,4′-(1,4-phenylene)bis(1-methylpyridinium) dichloride (**G2**) (Figure 5a), and bis(*N*-methylacridinium) nitrate (**G3**) (Figure 5b).

The change in the absorption of **1** with the addition of **G1** was monitored by UV-vis spectroscopy: the absorption at 311 nm gradually decreased and increased over a wide range up to 450 nm with a peak top at 330 nm (Figure 4b). This change in absorption appears to be a characteristic of an intermolecular charge-transfer transition between the CPP macroring of **1** and guest molecule, which is also supported by the DFT calculations (Figure 4b). Comparison of the relative Gibbs energy of **1⊃G1** with other conformations (e.g. bridging, riding, or exterior complexations) using the DFT calculations considering solvation effects of water by SMD solvation model revealed that the conformation in which **G1** is inside the CPP macroring is more stable than the other conformations over 16 kcal mol^{-1} (see Supporting Figure S49). The fluorescence titration revealed a linear decay in the fluorescence intensity of **1** upon the addition of **G1** (Figure 4c), which would be attributed to intermolecular photoinduced electron transfer. Furthermore, an isosbestic point was observed at 325 nm in the UV/vis titrations (Figure 4b), suggesting the formation of 1:1 complex, which is supported by the fact that in the Job's plot, the peak top was observed at a mole fraction of 0.5 (see Supporting Figure S31). The profiling of the change in absorbance at 312 nm fitted well with the curve fitting[34][35][36] using the 1:1 association model, and an association constant (K_a) at 298 K was estimated to be $5.4\pm0.8\times10^4$ M^{-1}.[37] The thermodynamic parameters were calculated from the van't Hoff plot (Figure 4b, inset) by using the results of variable-temperature UV-vis titrations, which were estimated to be $\Delta G°$ = –6.3 kcal mol^{-1} (298 K), $\Delta H°$ = –7.5 kcal mol^{-1} and $\Delta S°$ = –3.8 cal mol^{-1} K^{-1}.

These values are in close agreement with those acquired from the Isothermal Titration Calorimetry (ITC) measurements (Figure 4e).

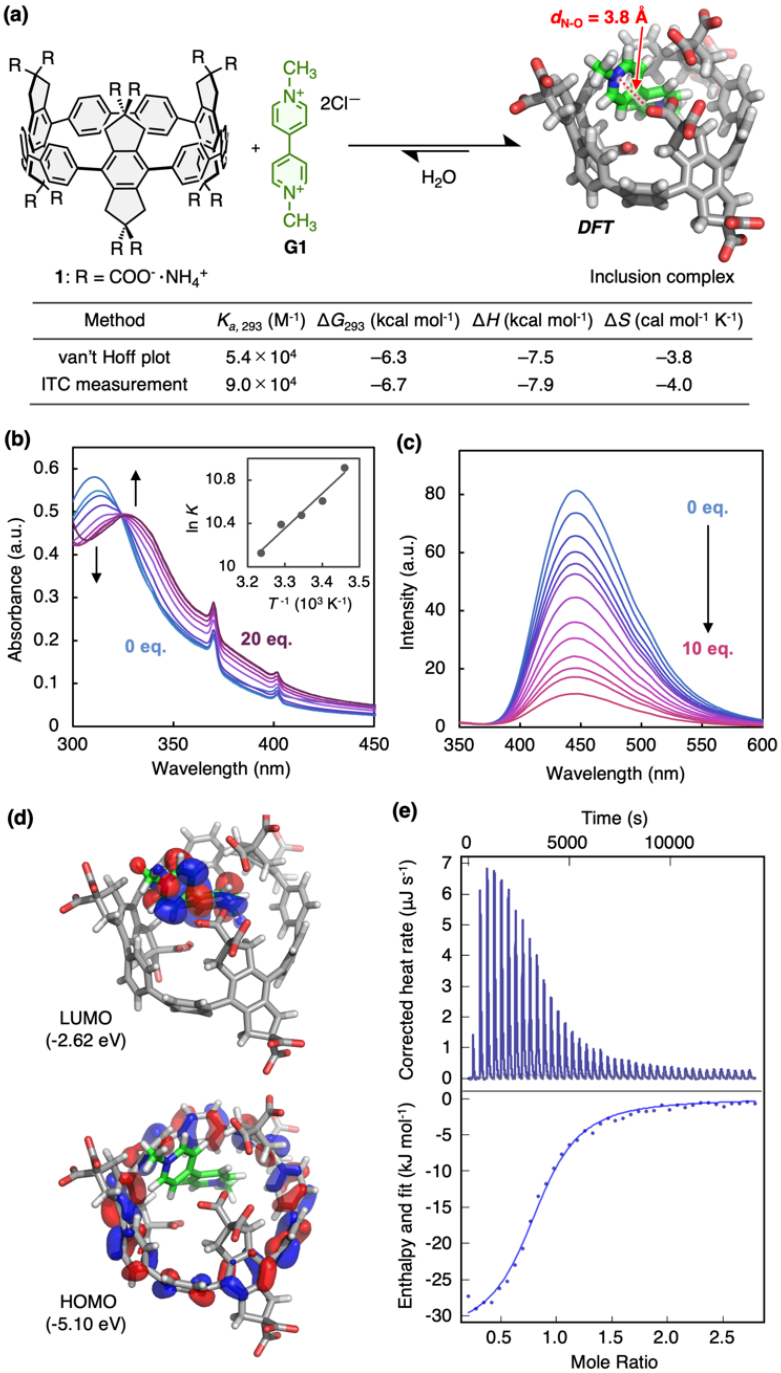

Method	$K_{a,293}$ (M^{-1})	ΔG_{293} (kcal mol^{-1})	ΔH (kcal mol^{-1})	ΔS (cal mol^{-1} K^{-1})
van't Hoff plot	5.4×10^4	–6.3	–7.5	–3.8
ITC measurement	9.0×10^4	–6.7	–7.9	–4.0

Figure 4. (a) Formation of inclusion complex between WS-[9]CPP (**1**) and methyl viologen dichloride (**G1**). The molecular structure of inclusion complex was simulated by DFT calculations (SMD-r^{2}SCAN-3c(+ma) level of theory). (b) UV/Vis titrations of **1** with **G1** (H_2O, [**1**] = 1.0 x 10^{-6} M, r.t.) (inset: van't Hoff plot). (c) Fluorescence titrations of **1** with **G1** (H_2O, [**1**] = 1.0 x 10^{-6} M, r.t.). (d) Kohn-Sham orbitals of inclusion complex (SMD-r^{2}SCAN-3c(+ma) level of theory) (Iso surface = 0.02). (e) Isothermal Titration Calorimetry (ITC) plots of **1** with **G1** (H_2O, [**1**] = 2.0 x 10^{-4} M, r.t.).

The large negative $\Delta H°$ value indicate that the inclusion proceeded in an enthalpy-driven process, mainly due to the intermolecular interactions. The non-covalent interaction (NCI) analyses using NCIPLOT[38] programs demonstrated the formation of intermolecular CH…π interactions and π-π stacking between **1** and **G1** (see Supporting Figure S50). In addition, the fact that $\Delta S°$ value is close to zero despite bimolecular association, suggests that desolvation of water molecules from the hydrophobic cavity also contributes to the formation of the inclusion complex. Based on the results of conformational search using CREST at the GFN-FF level and structural re-optimization through DFT calculations using CENSO,[39] it was found that the most stable conformation involves **G1** being encapsulated inside the CPP macroring. A carboxylate oxygen of **1** and a nitrogen atom of **G1** are in close proximity to each other, within a range of 3.8 Å (Figure 4a). These results indicate that the fixing of the carboxylates at the 2,6-positions of the hydrindacene units not only renders the CPP water-soluble, but also facilitates the formation of electrostatic interactions between the carboxylates on the inner side of the CPP macroring and the guest molecule, thereby promoting guest inclusion in an aqueous environment.

On the other hand, in the guest inclusion with **G2**, the ^{1}H NMR titration and Job's plot indicated the formation of a 1:2 inclusion complex (Figure 5a, also see Supporting Figures S39-41). The interaction parameter ($\alpha = 4\times K_{12}/K_{11}$) was calculated from the stepwise association constants (K_{11} = 4.1±1.2 × 10^3 M^{-1}, K_{12} = 2.4±0.1 × 10^3 M^{-1}), as determined by ^{1}H NMR titration, to be 2.3, suggesting that the formation of inclusion complex exhibits a weak positive cooperativity.[31] The association with **G3** occurred at 1:1 ratio with an association constant of 2.5 ± 0.1 × 10^3 M^{-1} (Figure 5b, also see Supporting Figures S44-46).

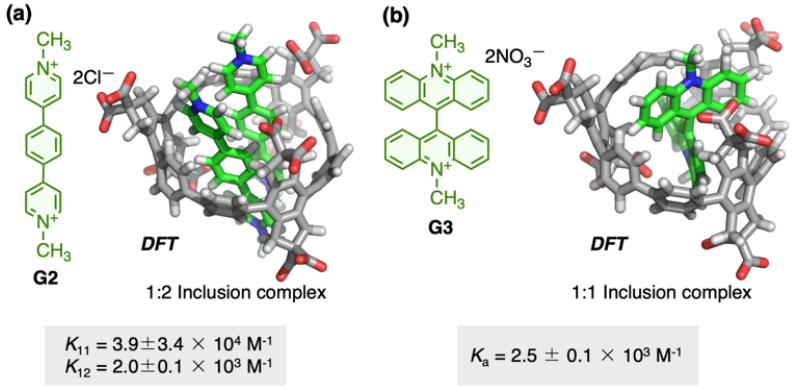

Figure 5. Optimized molecular structures of (a) 1:2 inclusion complex between **1** and **G2**, and (b) 1:1 inclusion complex between **1** and **G3**. These structures represent the most energetically stable conformations among the candidates obtained through conformational search using CREST at the GFN-FF level followed by structural optimization (SMD-r^{2}SCAN-3c(+ma) level of theory).

In the previous studies of the host-guest chemistry of [*n*]CPPs in organic solvents,[40] [*n*]CPPs show inclusion ability only for guest molecules with curved π-conjugated systems, such as fullerenes,[41] [*n*]CPPs with small ring size,[42] and a disk-shaped molecule,[43] alkyl chain with electron-withdrawing groups,[24] due to the attractive interactions such as π-π stacking and CH-π interactions. The water-soluble [9]CPP synthesized in this study exhibits the ability to encapsulate cationic guest molecules of diverse shapes in aqueous media, a remarkable finding that distinguishes it from the previous studies on host-guest chemistry of [*n*]CPPs in organic solvents.

The water-soluble corral[5]arene (Figure 1a, right) reported by Guo and Cai et al. [8] showed high inclusion ability (~10^{11} M^{-1}), which arises from the induced fit process based on the structural change of the host molecule associated with the guest inclusion. The CPP-based water-soluble supramolecular host in this study has a rigid macrocyclic framework that allows for the inclusion of up to two cationic guest molecules into the cavity. Such 1:2 inclusion behavior tends to be observed even in rigid supramolecular hosts such as cucurbit[*n*]uril,[44][45] however, WS-[9]CPP (**1**) has characteristic photophysical properties (e.g. visible fluorescence with high brightness) owing to the circular π-conjugated system. Therefore, WS-[9]CPP (**1**) holds promise for various applications, such as logic gate-based molecular photosensors[46][47] that can simultaneously recognize two different guest molecules, and the construction of complicated molecular machines driven in aqueous or biological media.[48]

Conclusions

In this study, we have successfully synthesized a water-soluble [9]cycloparaphenylene derivative containing twelve ammonium carboxylates *via* a macrocyclic gold complex. To the best of our knowledge, this is the first example of CPP derivative that is completely soluble in pure water. Moreover, this molecule exhibits strong visible fluorescence in water (λ_{em} = 447 nm, φ_F = 0.64, brightness ($\varepsilon \times \varphi_F$) = 5.1×10^4) and shows the ability to encapsulate various guest molecules with alkyl pyridinium salts in aqueous media, as indicated by a change in visible fluorescence. Currently, we are engaged in the development of the potential application of these novel water-soluble supramolecular host with strong visible fluorescence in water.

Conflicts of interest

The authors declare no conflicts of interest.

Author Contributions Y.T. and H.K. conceived the project. R.M. synthesized and characterized all compounds and evaluated their photophysical and host-guest properties. T.K. and K.S. exploited a

synthetic route toward the hydrindacene derivative with diiodo group (**7**). T.I. conducted all the theoretical calculations. Y.T. carried out X-ray crystallographic measurements and analysis. Y.T. drafted the initial manuscript, while H.K. and K.O. subsequently revised it.

Acknowledgements

This work was financially supported by a Grant-in-Aid for Young Scientists (JSPS KAKENHI grant number JP19K15533 for Y.T.), Grants-in-Aid for Scientific Research (C) (JSPS KAKENHI grant number 21K05093 for K.O.), Grants-in-Aid for Transformative Research Area (A) "*Condensed Conjugation*" (JSPS KAKENHI grant numbers 21H05496 for Y.T. and 23H04041 for Y.T.). Y.T. gratefully acknowledges Tokyo University of Science Grant for Young or Female Researchers. The computation was partly performed using Research Center for Computational Science, Okazaki, Japan (Project: 22-IMS-C158 for T.I.).

Notes and references

[1] M. Ueno, T. Tomita, H. Arakawa, T. Kakuta, T. aki Yamagishi, J. Terakawa, T. Daikoku, S. ichi Horike, S. Si, K. Kurayoshi, C. Ito, A. Kasahara, Y. Tadokoro, M. Kobayashi, T. Fukuwatari, I. Tamai, A. Hirao, T. Ogoshi, *Commun. Chem.* **2020**, *3*, 183.

[2] Z. Li, N. Song, Y. W. Yang, *Matter* **2019**, *1*, 345–368.

[3] T. Ogoshi, M. Hashizume, T. A. Yamagishi, Y. Nakamoto, *Chem. Commun.* **2010**, *46*, 3708–3710.

[4] G. Yu, M. Xue, Z. Zhang, J. Li, C. Han, F. Huang, *J. Am. Chem. Soc.* **2012**, *134*, 13248–13251.

[5] Q. Duan, F. Wang, K. Lu, *Front. Chem.* **2022**, *10*, 973313.

[6] A. P. Davis, *Chem. Soc. Rev.* **2020**, *49*, 2531–2545.

[7] L. Catti, R. Sumida, M. Yoshizawa, *Coord. Chem. Rev.* **2022**, *460*, 214460.

[8] R. Wang, W.-B Li, J.-Y. Deng, H. Han, F.-Y. Chen, D.-Y. Li, L.-B. Jing, Z. Song, R. Fu, D.-S. Guo, K. Cai, *Angew. Chem. Int. Ed.* **2024**, *64*, e202317402.

[9] S. Yamago, E. Kayahara, T. Iwamoto, *Chem. Rec.* **2014**, *14*, 84–100.

[10] E. R. Darzi, R. Jasti, *Chem. Soc. Rev.* **2015**, *44*, 6401–6410.

[11] Y. Segawa, A. Yagi, K. Matsui, K. Itami, *Angew. Chem. Int. Ed.* **2016**, *55*, 5136–5158.

[12] B. M. White, Y. Zhao, T. E. Kawashima, B. P. Branchaud, M. D. Pluth, R. Jasti, *ACS Cent. Sci.* **2018**, *4*, 1173–1178. The photophysical properties of the compound shown in Figure 1b are as follows: λ_{em} = 510 nm, φ_F = 0.17, brightness ($\varepsilon \times \varphi_F$) = 0.99×10^4.

[13] H. Kawai, T. Utamura, E. Motoi, T. Takahashi, H. Sugino, M. Tamura, M. Ohkita, K. Fujiwara, T. Saito, T. Tsuji, T. Suzuki, *Chem. -Eur. J.* **2013**, *19*, 4513–4524.

[14] H. Kawai, R. Katoono, K. Nishimura, S. Matsuda, K. Fujiwara, T. Tsuji, T. Suzuki, *J. Am. Chem. Soc.* **2004**, *126*, 5034–5035.

[15] H. Kawai, R. Katoono, K. Fujiwara, T. Tsuji, T. Suzuki, *Chem. Eur. J.* **2005**, *11*, 815–824.

[16] H. Kawai, *Bull. Chem. Soc. Jpn.* **2015**, *88*, 399–409

[17] H. Kawai, T. Umehara, K. Fujiwara, T. Tsuji, T. Suzuki, *Angew. Chem. Int. Ed.* **2006**, *45*, 4281–4286.

[18] T. Umehara, H. Kawai, K. Fujiwara, T. Suzuki, *J. Am. Chem. Soc.* **2008**, *130*, 13981–13988.

[19] H. Sugino, H. Kawai, T. Umehara, K. Fujiwara, T. Suzuki, *Chem. Eur. J.* **2012**, *18*, 13722–13732.

[20] H. Sugino, H. Kawai, K. Fujiwara, T. Suzuki, *Chem. Lett.* **2012**, *41*, 79–81.

[21] S. Hoshino, K. Ono, H. Kawai, *Front. Chem.* **2022**, *10*, 885939.

[22] Y. Tsuchido, R. Abe, T. Ide, K. Osakada, *Angew. Chem. Int. Ed.* **2020**, *59*, 22928–22932.

[23] Y. Yoshigoe, Y. Tanji, Y. Hata, K. Osakada, S. Saito, E. Kayahara, S. Yamago, Y. Tsuchido, H. Kawai, *JACS Au* **2022**, *2*, 1857–1868.

[24] N. Narita, Y. Kurita, K. Osakada, T. Ide, H. Kawai, Y. Tsuchido, *Nat. Commun.* **2023**, *14*, 8091.

[25] P. Holý, M. Havránek, M. Pánková, L. Ridvan, J. Závada, *Tetrahedron* **1997**, *53*, 8195–8210.

[26] V. K. Chaikovskii, V. D. Filimonov, A. A. Funk, V. I. Skorokhodov, V. D. Ogorodnikov, *Russ. J. Org. Chem.* **2007**, *43*, 1291–1296.

[27] W. J. Wolf, M. S. Winston, F. D. Toste, *Nat. Chem.* **2014**, *6*, 159–164.

[28] S. Karcher, A. Kornmüller, M. Jekel, *Wat. Res.* **2001***, 35,* 3309–3316.

[29] T. Ogoshi, A. Harada, *Sensors* **2008***, 8,* 4961–4982.

[30] F. Neese, *Wiley Interdiscip. Rev. Comput. Mol. Sci.* **2012**, *2*, 73–78.

[31] Y. Segawa, A. Fukazawa, S. Matsuura, H. Omachi, S. Yamaguchi, S. Irle, K. Itami, *Org. Biomol. Chem.* **2012**, *10*, 5979–5984.

[32] V. S. Reddy, C. Camacho, J. Xia, R. Jasti, S. Irle, *J. Chem. Theory Comput.* **2014**, *10*, 4025–4036.

[33] L. Adamska, I. Nayyar, H. Chen, A. K. Swan, N. Oldani, S. Fernandez-Alberti, M. R. Golder, R. Jasti, S. K. Doorn, S. Tretiak, *Nano Lett.* **2014**, *14*, 6539–6546.

[34] Bindfit, *http://supramolecular.org*

[35] P. Thordarson, *Chem. Soc. Rev.* **2011**, *40*, 1305–1323.

[36] D. Brynn Hibbert, P. Thordarson, *Chem. Commun.* **2016**, *52*, 12792–12805.

[37] The ^{1}H NMR titration profile (Figure S27) displayed a sigmoidal curve, consistent with a 1:2 binding model, with association constants determined as $K_{11} = 3.9 \pm 3.4 \times 10^{4}$ M^{-1} and $K_{12} = 2.0 \pm 0.1 \times 10^{3}$ M^{-1} (it should be noted that the error associated with K_{11} was relatively high). The

significant difference between K_{11} and K_{12} implies that the initial step primarily governs the association between **1** and **G1**. In addition, UV/vis titrations (Figures S30, S32-37), Job's plot (Figure S31), and ITC measurement (Figure 38), suggest the formation of 1:1 inclusion complex. Based on these results, we discuss the equilibrium of **1** and **G1** as a pseudo 1:1 association.

[38] E. R. Johnson, S. Keinan, P. Mori-Sánchez, J. Contreras-García, A. J. Cohen, W. Yang, *J. Am. Chem. Soc.* **2010**, *132*, 6498–6506.

[39] S. Grimme, F. Bohle, A. Hansen, P. Pracht, S. Spicher, M. Stahn, *J. Phys. Chem. A* **2021**, *125*, 4039–4054.

[40] D. Lu, Q. Huang, S. Wang, J. Wang, P. Huang, P. Du, *Front. Chem.* **2019**, *7*, 668.

[41] T. Iwamoto, Y. Watanabe, T. Sadahiro, T. Haino, S. Yamago, *Angew. Chem. Int. Ed.* **2011**, *50*, 8342–8344.

[42] S. Hashimoto, T. Iwamoto, D. Kurachi, E. Kayahara, S. Yamago, *ChemPlusChem* **2017**, *82*, 1015–1020.

[43] S. Adachi, M. Shibasaki, N. Kumagai, *Nat. Commun.* **2019**, *10*, 3820.

[44] F. Tian, D. Jiao, F. Biedermann, O. A. Scherman, *Nat. Commun.* **2012**, *3*, 1207.

[45] Y. Liu, H. Yang, Z. Wang, X. Zhang, *Chem. Asian J.* **2013**, *8*, 1626–1632.

[46] L. Liu, P. Liu, L. Ga, J. Ai, *ACS Omega* **2021**, *6*, 30189–30204.

[47] S. Erbas-Cakmak, S. Kolemen, A. C. Sedgwick, T. Gunnlaugsson, T. D. James, J. Yoon, E. U. Akkaya, *Chem. Soc. Rev.* **2018**, *47*, 2228–2248.

[48] T. G. Johnson, M. J. Langton, *J. Am. Chem. Soc.* **2023**, *145*, 27167–27184.